Paper AAS 03-536

Artificial Gravity and Abort Scenarios via Tethers for Human Missions to Mars

Michael Jokic
School of Engineering
The University of Queensland
Brisbane, QLD
Australia

James M. Longuski
School of Aeronautics and Astronautics
Purdue University
West Lafayette, Indiana

AAS/AIAA Astrodynamics Specialists Conference

Big Sky, Montana **August 3-7, 2003**

AAS Publications Office, P.O. Box 28130, San Diego, CA 92198

ARTIFICIAL GRAVITY AND ABORT SCENARIOS VIA TETHERS FOR HUMAN MISSIONS TO MARS

Michael D. Jokic* and James M. Longuski†

We develop minimum-mass tether designs for a rotating human transport, which not only provides artificial gravity but also the potential for free-return aborts. Our investigation reveals that severing the tether can provide a propellant-free boost to return astronauts to Earth in the event of an aborted landing on Mars. The years 2018 and 2020 are identified as good launch opportunities for propellant-free abort scenarios using Earth-Mars-Earth trajectories.

INTRODUCTION

One possible tether transport facility is depicted in Figure 1. The transport facility spins so that the astronauts in the habitat module experience an acceleration similar to the gravitational acceleration they normally experience on Earth. The momentum of the rotating tether system might be used to provide a propellant-free boost for returning the astronauts to Earth after an aborted Mars landing.

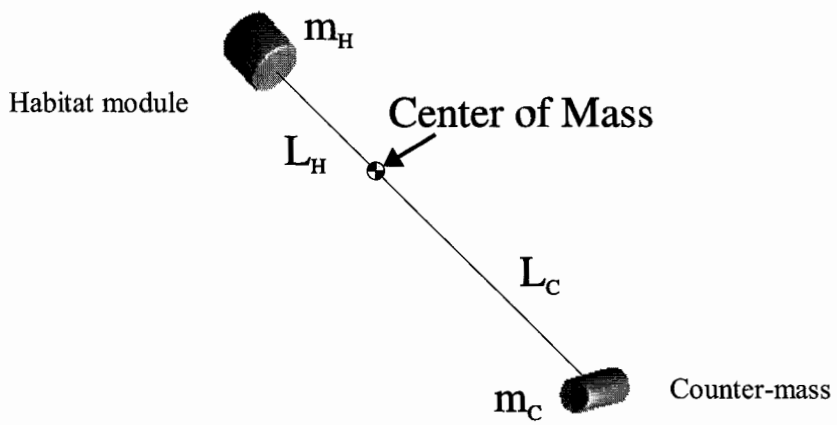

Figure 1 Possible configuration of space transport with artificial gravity.

* Ph.D. Candidate, School of Engineering, The University of Queensland, Australia, 4072. Member AIAA. m.jokic@uq.edu.au
† Professor, School of Aeronautics and Astronautics. Purdue University, West Lafayette, IN, 47907-2023. Member AAS, Associate Fellow AIAA. longuski@ecn.purdue.edu

Space-based tethered transportation systems can eliminate or reduce the need for expendable propellant.[1-5] Cosmo and Lorenzini[5] present an excellent overview of potential tether applications. For space-based systems, tapered tether designs minimize the mass and the structural loads.[5-9] Puig-Suari et al.[7] discuss the importance of minimizing the mass for a tether sling transportation system. Jokic and Longuski[9] extend this work by designing tether slings stationed on Phobos for human transportation systems between Earth and Mars.

Possible scenarios for human missions to Mars are widely discussed in the literature.[10-40] The work by Lyne and Townsend[25] details a powered swingby scenario to return astronauts safely to Earth in the event of an aborted Mars landing. Okutsu and Longuski[29] present an investigation of possible free-return trajectories (requiring no propellant expenditure after launch). Their work identifies a potential Earth-Mars-Venus-Earth (EMVE) trajectory with desirable mission parameters in 2014.

In this paper, we develop minimum-mass designs for the tether in a human transport with artificial gravity. We outline a general methodology for designing a minium-mass tethered system in a configuration consisting of two end masses connected by a tether, as shown in Figure 1. We then discuss trajectories with abort capabilities for human missions to Mars. Our analysis identifies some potential trajectories that can use the momentum of the spinning tethered transport to provide the necessary boost to transfer astronauts back to Earth without the use of propellant.

ABORT SCENARIOS FOR HUMAN MISSIONS TO MARS

Our investigation aims to identify abort options for human missions to Mars for a worst-case scenario. Ideally, a mission to Mars will be configured to enable the astronauts to return to Earth without requiring an engine to provide a velocity change. Unfortunately, free-return trajectories do not conform to the needs of human missions for all potential launch years. We examine how a spinning tether transportation system might be able to provide the necessary velocity change to return astronauts to Earth. The primary role of tethered system is to generate an artificial gravity environment. By rotating the tethered transport, the astronauts in the habitat module experience a centrifugal acceleration equal in magnitude to the gravitational acceleration people would normally experience on Earth. Figure 2 shows how a rotating tethered transport system can provide the velocity change required for an Earth-Mars-Earth (E-M-E) abort trajectory. The tether connecting the habitat and counter-mass modules is severed near apoapse so that the habitat has the velocity needed to return the astronauts to Earth. The specific abort scenario depicted in Figure 2 is one of the solutions we examine in this paper.

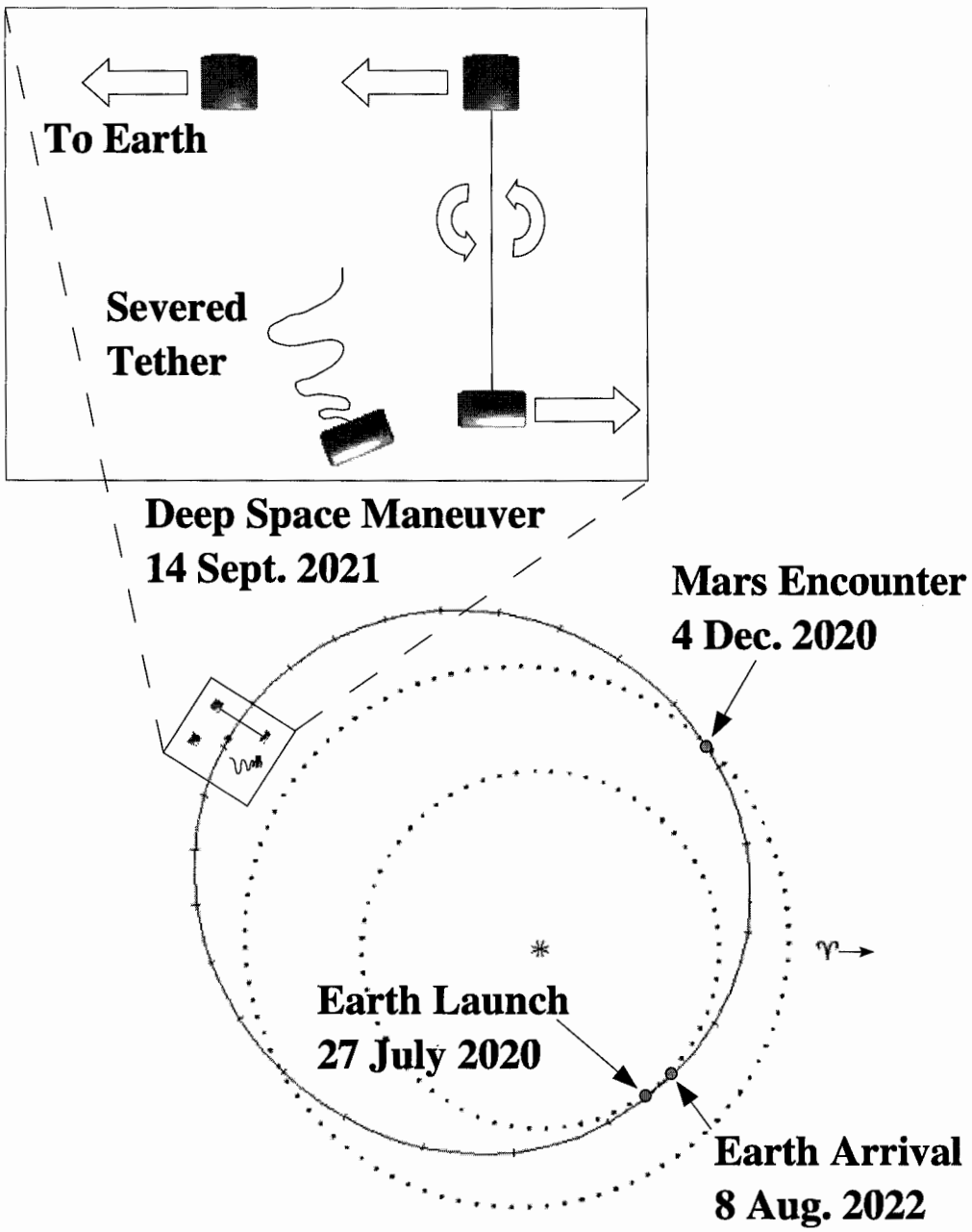

Figure 2 An aborted mission to Mars via an E-M-E trajectory with a ΔV achieved by severing the tether.

We refer to NASA's Design Reference Mission (DRM) to define some of the tethered transport's mass. Our analysis assumes that the masses at the end of the tether correspond to the crew-lander-entry mass (habitat module) and the crew-lander, Nuclear Thermal Rocket (NTR) mass (counter-mass). Some of the masses specified in the DRM

are shown in Table 1. One possible alternative tethered transport design might consist of the crew-lander-entry mass tethered to the cargo-lander-entry mass. The emphasis of our examination is on propellant-free abort options, which represent worst-case scenarios where the engines on the descent stage fail. If the systems associated with the decent engines do not fail, the masses specified in the DRM suggest that a velocity change of 0.77 km/s is possible. The E-M-E abort trajectory depicted in Figure 2 requires a 0.5 km/s velocity change near periapse to return the habitat module to Earth. Our tether transport design does not require the descent engines to return the habitat module to Earth but the engines are also capable of producing a boost of 0.5 km/s.

Table 1: System masses for Human Missions to Mars[23]

System	Mass, kg
Crew-Lander Entry Mass	60,806
Crew-Lander NTR system	26,600
Crew-Lander TMI Propellant	50,000
Cargo-Lander Entry Mass	66,043
Cargo-Lander NTR system	23,400
Cargo-Lander TMI Propellant	45,300

MINIMUM TETHER MASS DESIGNS FOR ARTIFICIAL GRAVITY

Design Methodology

Our design methodology for the minimum-mass configuration of the tethered transport begins with a specified value for the speed of the habitat module, relative to the system's center of mass (V_H). For a tether material with a characteristic velocity determined using[7]

$$V_{CHAR} = \sqrt{\frac{2\sigma}{\rho}} \tag{1}$$

We define the non-dimensional velocity of the habitat module as

$$V_H^* = V_H / V_{CHAR} \tag{2}$$

The length of the tether from the transport's center of mass to the habitat module is independent of the velocity. Thus we can specify the tether length by constraining the acceleration (for a given V_H):

$$L_H = V_H^2 / a_{MAX} \tag{3}$$

where, a_{MAX} is the maximum acceleration experienced by astronauts in the habitat. For the case where the counter mass is equal to the habitat mass, the total length of the tether is simply twice the length, L_H. In general, however, the end masses are not equal and the length L_C is dependent on L_H, V_H and m_C. To determine L_C we apply the definition of the center of mass for collinear mass elements, with the center of mass defined at the origin

$$m_H L_H + \int_0^{L_H} \rho A_{x,H} x \, dx - m_C L_C - \int_0^{L_C} \rho A_{x,C} x \, dx = \sum_{i=1}^{n} x_i m_i = 0 \tag{4}$$

where, x_i is the distance from the center of mass, $A_{x,C}$ and $A_{x,H}$ represent the minimum cross-sectional area of the tether at location x between the system's center of mass and the counter-mass or habitat mass, and m_i is the mass of an element. By evaluating the integrals and performing the necessary algebra, Eq. (4) becomes

$$m_H L_H \exp\left(V_H^{*2}\right) = m_C L_C \exp\left(V_H^{*2} L_C^2 / L_H^2\right) \tag{5}$$

Rearranging for L_C produces

$$L_C = m_H L_H \Big/ m_C \exp\left\{V_H^{*2} - \tfrac{1}{2} \mathrm{W}\left[2 V_H^{*2} m_H^2 \exp\left(V_H^{*2}\right) / m_C^2\right]\right\} \tag{6}$$

where W(z) is the Lambert W function[41] defined as the solution of

$$z = \mathrm{W}(z) \mathrm{e}^{\mathrm{W}(z)} \tag{7}$$

With L_C determined, the velocity of the counter-mass relative to the transport's center of mass is calculated by

$$V_C = \left(V_H / L_H\right) L_C \tag{8}$$

and the nondimensional velocity of the counter-mass is determined from

$$V_C^* = V_C / V_{CHAR} \tag{9}$$

The mass associated with the tether lengths, L_H and L_C , are defined in terms of the nondimensional velocities and the error function as[7]

$$m_{T,H} = m_H \sqrt{\pi} V_H^* \exp\left(V_H^{*2}\right) \mathrm{erf}\left(V_H^*\right) \tag{10}$$

and

$$m_{T,C} = m_C \sqrt{\pi}\, V_C^* \exp\left(V_C^{*2}\right) \mathrm{erf}\left(V_C^*\right) \tag{11}$$

respectively. Hence, the total minimum mass of the tether is found by adding the mass of the two sections, which is written as

$$m_{T,MIN} = m_{T,H} + m_{T,C} \tag{12}$$

Our final minimum-mass tether design is tapered from a maximum cross-sectional area at the center of mass to minimum cross-sectional areas at the ends.

Mass Performance

We now examine how the counter-mass-to-habitat-mass ratio and the relative velocity of the habitat, V_H, affect the mass of the tether. The material selected for the analysis is Zylon, which has a tensile strength of 5.8 GPa and a density of 1560 kg/m^3. Substituting these properties into Eq. (1) reveals that the characteristic speed of Zylon is 2.7 km/s, which is the maximum tip speed that a non-tapered tether can support before failure. For comparison, we determine the propellant mass required to produce the desired change in the habitat module's velocity using a single-stage rocket model with an I_{sp} of 379 s.

Figure 3 shows the ratio of the tether-mass-to-propellant-mass (m_T/m_P) for a range of habitat throw velocities and ratios of counter-mass-to-habitat-mass (m_C/m_H). The mass of the tether is highly dependent on the desired habitat throw velocity, so m_T/m_P increases very quickly with increasing throw velocity. As expected, higher values of m_C/m_H for a particular habitat throw velocity produce smaller tether masses and, subsequently, smaller m_T/m_P. Ideally, m_T/m_P should be less than unity so that the mass of the tether is less than the propellant required to complete a particular abort trajectory. For an m_C/m_H value of 0.5, this condition requires that the habitat throw velocity must be less than about 0.33 km/s. A mass ratio of 0.3 requires a change in velocity of less than 0.24 km/s to keep the m_T/m_P ratio less than one. If the mass available for the tether transport is assumed to match the Mars Design Reference Mission (DRM), m_C/m_H is about 0.43. A value of m_T/m_P greater than one is not necessarily a reason to dismiss a design as the system has the added benefit of generating artificial gravity and reducing the entry velocity of the habitat for aerobraking. The habitat module's entry velocity is reduced by severing the tether so that the module is released in the opposite direction to the transport's flight path. A lower entry velocity decreases the mass required for heat shielding.

The ratio of the tether-mass-to-habitat-mass (m_T/m_H) is also investigated as a function of the habitat throw velocity and m_C/m_H. Figure 4 contains curves illustrating the dependency of m_T/m_H on the required habitat throw velocity. For m_C/m_H values of 0.5 and 0.3, the tether mass remains less than half the habitat mass ($m_T/m_H < 0.5$) for habitat throw velocities less than 0.81 and 0.75 km/s, respectively. The performance of the tethered transport, in terms of mass, is highly dependent on the required habitat

throw velocity (V_H), the strength-to-weight ratio of the tether material and the ratio of the end masses (m_C/m_H).

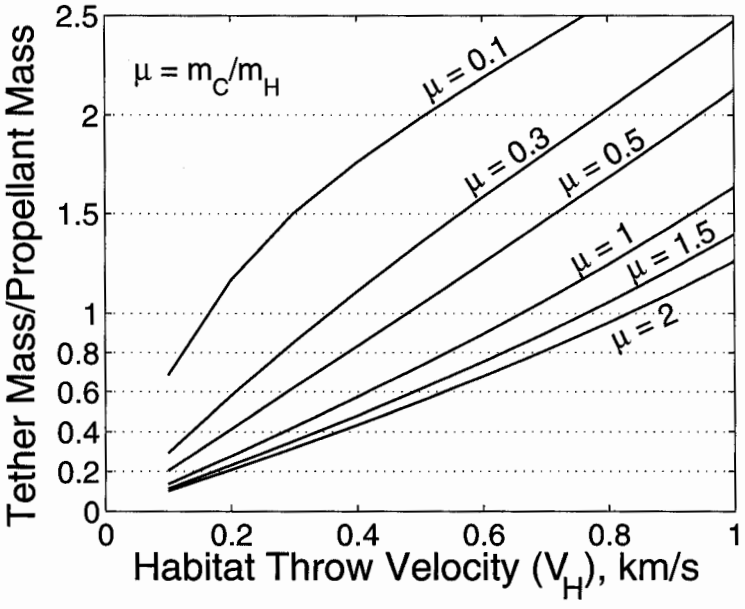

Figure 3 Tether-mass-to-propellant-mass ratio versus required habitat velocity.

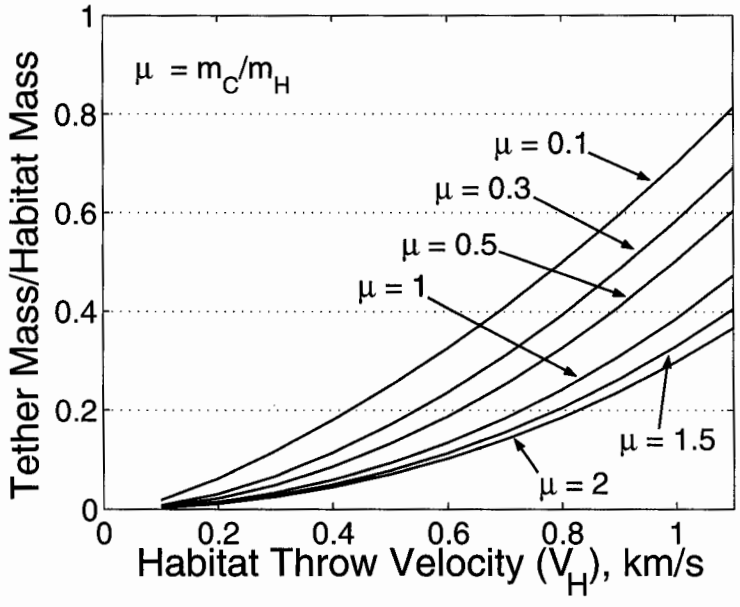

Figure 4 Tether-mass-to-habitat-mass ratio versus required habitat velocity.

ABORT OPTIONS VIA TETHERS

We seek trajectories in which a small ΔV can return astronauts to Earth in an acceptable time of flight. If the ΔV is small enough, then our tether design can achieve the maneuver with minimal mass. The spinning tether system has the added benefit of generating an artificial gravity environment. We only allow the ΔV to occur after the tether transport reaches Mars. For our analysis, we design the tether transport so that the acceleration experienced by the astronauts in the habitat is equal to the acceleration on the surface of the Earth (1g).

Table 2 contains some of our constraints for identifying acceptable abort options. We use the conditions to examine Earth-Mars-Earth (E-M-E), Earth-Mars-Venus-Earth (E-M-V-E) and Earth-Venus-Mars-Earth (E-V-M-E) trajectory paths between 2014 and 2031. The constraints listed are in decreasing order of priority. The first three are presented in the literature as practical design limits for Mars missions. Times of flight longer than those listed in Table 2 will not have a significant detrimental effect on the health of the astronauts due to the artificial gravity environment of the tether transport. We assume an upper bound of 3 for m_T/m_P.

Table 2: Human mission constraints listed in order of decreasing priority

Mission Variable	Constraint
Launch V_∞[a]	≤ 4.5 km/s[23]
Mars Arrival V_∞	≤ 7.1 km/s[42]
Earth Arrival V_∞	≤ 9.3 km/s[42]
m_T/m_P	≤ 3
Time of Flight E-M	≤ 180 days[22]
Total Time of Flight	≤ 800 days[22]

[a]DRM in 2014 requires 3.32 km/s.[29] Value based on requirement for the 2024 180-day transfer and DRM vehicle masses.

Earth-Mars-Earth Trajectories

Patel et. al.[27] examine potential E-M-E free-return trajectories in some detail. Our investigation, however, allows for a small ΔV in the trajectory to ensure that the conditions of Table 2 are met. Table 3 contains the E-M-E options obtained for launch years between 2014 and 2028 via MIDAS.[44] There are no free-return solutions for our constraints. We note that 2018 and 2020 contain launch opportunities that closely match the mission constraints. The required deep space maneuvers of 0.71 and 0.5 km/s for the 2018 and 2020 cases can be achieved by severing the tether. Figure 2

depicts the 2020 abort scenario in detail. As we noted ealier, the 0.5 and 0.71 km/s deep space maneuvers (DSM) can be achieved by expending the propellant stored on the transport for descent to the surface of Mars. In all of the cases presented, the time of flight (TOF) to return to Earth is less than the imposed 800-day limit.

Table 4 shows the tether designs needed to achieve the deep space maneuvers of the E-M-E abort trajectories. The mass ratio, m_T/m_p, for the 2018 and 2020 cases are 2.3 and 1.6, respectively. Our 2018 and 2020 solutions require tether lengths of 187 and 134 km. Only the opportunities identified in 2018, 2020 and 2028 have a tether mass which is less than half the habitat mass ($m_T/m_H < 0.5$). We also identified opportunities in 2026 and 2028, which meet our mass ratio limit for the tether but the arrival velocities at Mars are larger than the established 7.1 km/s constraint.

Table 3: E-M-E abort options with a deep space maneuver

Launch Date, yyyy/mm/dd	Launch V_∞, km/s	Mars Arrival V_∞, km/s	Earth Arrival V_∞, km/s	Deep Space Maneuver, km/s	TOF to DSM, days	TOF to Mars,[a] days	TOF to Earth,[b] days
2014/01/06	3.71	8.07	4.65	1.32	455	160	775
2016/02/28	3.45	7.58	4.79	1.20	493	125	778
2018/05/10	**3.90**	**7.09**	**5.06**	**0.71**	**491**	**187**	**759**
2020/07/27	**4.50**	**5.59**	**5.01**	**0.50**	**418**	**134**	**742**
2022/09/12	4.52	4.94	4.90	1.01	443	171	753
2024/10/17	4.56	6.07	4.86	1.12	448	180	753
2026/11/21	4.51	7.83	4.85	0.91	443	172	747
2028/12/28	4.51	9.53	4.86	0.64	437	160	741

[a] TOF to Mars is the time of flight for E-M.
[b] TOF to Earth is time of flight for E-M-E.

Table 4: Tether designs for E-M-E abort options

Launch Date, yyyy/mm/dd	Deep Space Maneuver, km/s	m_C/m_H	Tether Mass (m_T), Mg	Tether Length (L_C+L_H), km	m_T/m_H	m_T/m_p
2014/01/06	1.32	0.44	81.2	461	1.3	4.5
2016/02/28	1.20	0.44	66.8	388	1.1	4.0
2018/05/10	**0.71**	**0.44**	**24.2**	**150**	**0.40**	**2.3**
2020/07/27	**0.50**	**0.44**	**12.5**	**77.8**	**0.21**	**1.6**
2022/09/12	1.01	0.44	47.4	284	0.78	3.3
2024/10/17	1.12	0.44	58.1	343	0.96	3.7
2026/11/21	0.91	0.44	38.8	236	0.64	2.9
2028/12/28	0.64	0.44	19.9	123	0.33	2.1

Earth-Mars-Venus-Earth Trajectories

We searched for possible E-M-V-E abort trajectories using STOUR,[43] a patched-conic propagator. Figure 5 presents the trajectories found between 2014 and 2031 with a launch hyperbolic excess speed (V_∞) of 4.5 km/s. We searched for viable trajectories, which require a launch V_∞ between 3.4 and 4.6 km/s using an increment of 0.1 km/s. The cases with a launch V_∞ of 4.5 km/s are represented in Figure 5 because this is the upper limit determined for the DRM configuration and to ensure clarity. Despite the large number of solutions available in 2014 and 2032, allowing for small ΔV does not result in opportunities in all launch years. Our search does not reveal any potential trajectories in 2022 and 2028. A large number of trajectories requiring little, or no, ΔV are shown in Figure 6. All of the trajectories reported in Figure 6 meet our design requirements including the V_∞ at Earth and Mars. We selected our final solutions from the STOUR output by displaying the data in graphs such as Figures 5 and 6.

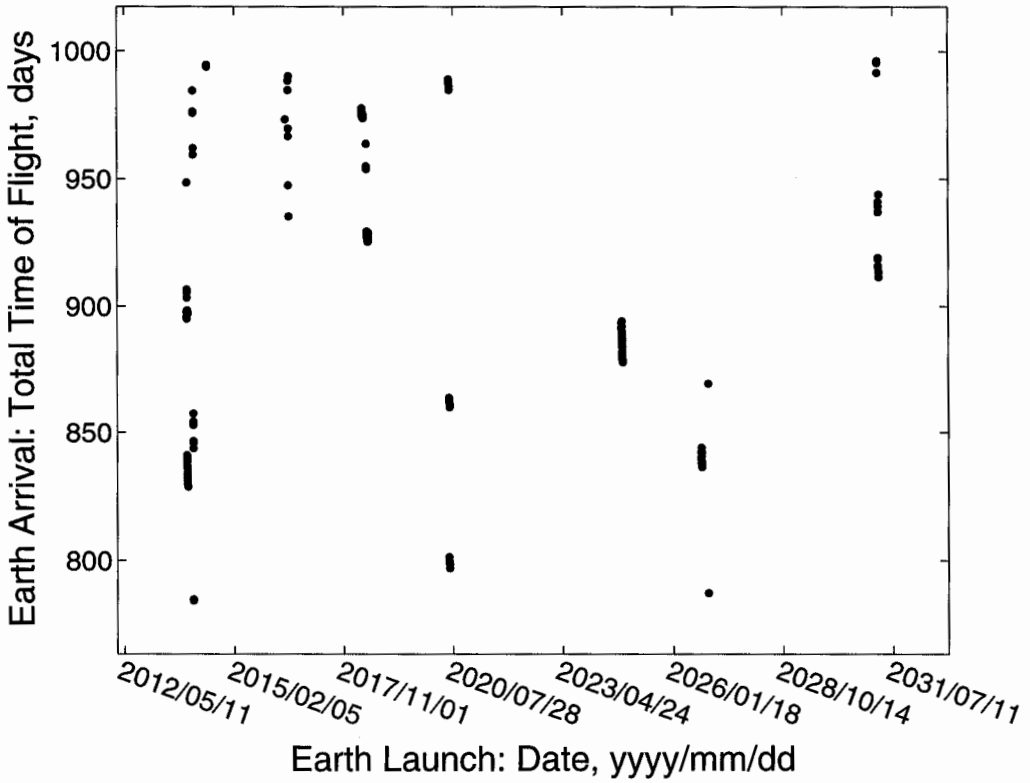

Figure 5 E-M-V-E trajectories found between 2014 and 2031 with a maximum time-of-flight of 1000 days. The minimum flyby altitude searched is 200 km with a launch V_∞ of 4.5 km/s and a maximum ΔV between Mars and Venus of 0.8 km/s.

Table 5 contains our best options for E-M-V-E abort trajectories between 2014 and 2031. We found opportunities in 2014 and 2020, which meet our design constraints. The 2014 abort option is a free-return scenario, which is in agreement with

the solution found by Okutsu and Longuski.[29] While the remaining trajectories listed in Table 5 violate the design constraints, the opportunity identified in 2024 only significantly exceeds the limits in the total time of flight (881 days). Table 6 lists the tether tranport designs corresponding to the reported E-M-V-E abort trajectories. There are no design requirements based on the 2014 trajectory as it represents a free-return option. The 2020 trajectory requires a ΔV of 0.76 km/s, which corresponds to a tether with a length of 170 km and a mass ratio m_T/m_p of 2.4.

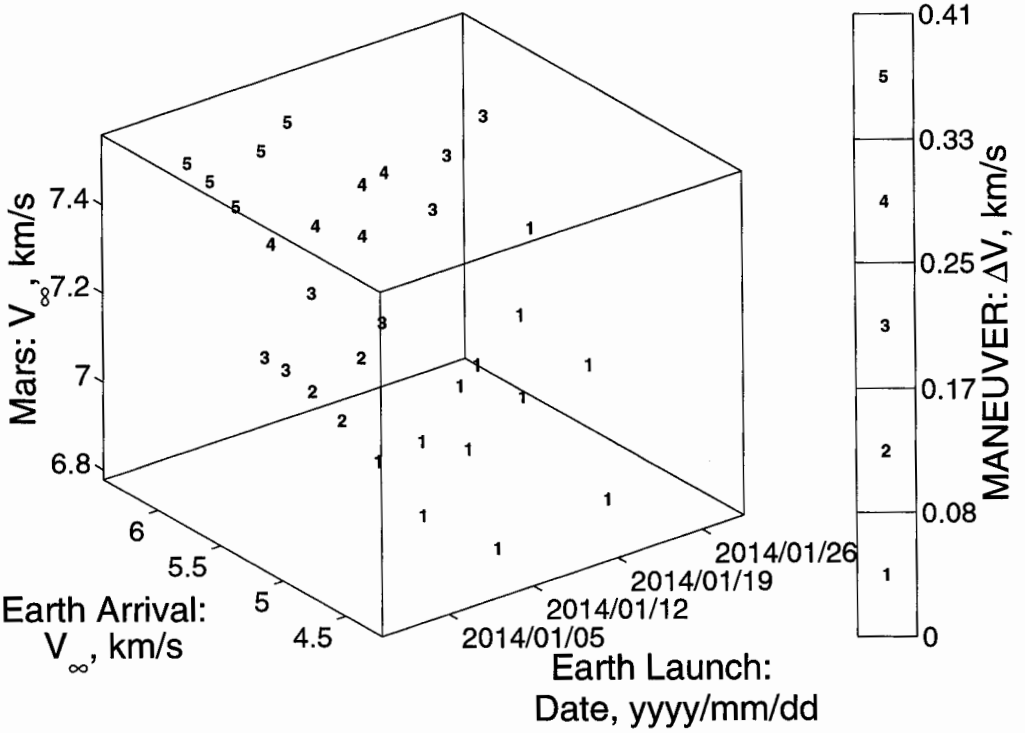

Figure 6 2014 E-M-V-E trajectory opportunities with TOF < 810 days.

Table 5: E-M-V-E abort options with a deep space maneuver

Launch Date, yyyy/mm/dd	Launch V_∞, km/s	Mars Arrival V_∞, km/s	Earth Arrival V_∞, km/s	Deep Space Maneuver, km/s	TOF to Mars,[a] days	TOF to Earth,[b] days
2014/01/13	**3.6**	**6.98**	**4.81**	**0.00**	**170**	**800**
2016/06/14	4.5	6.11	6.84	0.80	370	935
2016/11/29	4.3	4.95	10.4	0.78	200	791
2018/06/13	4.5	4.75	5.04	0.15	262	925
2020/06/24	**4.5**	**4.43**	**5.86**	**0.76**	**168**	**800**
2024/10/16	4.5	5.91	7.52	0.38	184	881
2026/10/07	4.3	4.35	8.63	0.79	263	835
2031/03/01	4.5	7.07	5.32	0.48	380	912

[a] TOF to Mars is the time of flight for E-M.
[b] TOF to Earth is time of flight for E-M-V-E.

Table 6: Tether designs for E-M-V-E abort options

Launch Date, yyyy/mm/dd	Deep Space Maneuver, km/s	m_C/m_H	Tether Mass (m_T), Mg	Tether Length (L_C+L_H), km	m_T/m_H	m_T/m_p
2014/01/13	**0.00**	**0.44**	a	a	a	a
2016/06/14	0.80	0.44	30.3	186	0.50	2.6
2016/11/29	0.78	0.44	28.9	178	0.48	2.5
2018/06/13	0.15	0.44	1.20	7.47	0.02	1.2
2020/06/24	**0.76**	**0.44**	**27.5**	**170**	**0.45**	**2.4**
2024/10/16	0.38	0.44	7.38	46.1	0.12	1.3
2026/10/07	0.79	0.44	29.6	182	0.49	2.5
2031/03/01	0.48	0.44	11.5	72.0	0.19	1.6

[a] There are no geometric requirements for the tether when the deep space maneuver is zero.

Earth-Venus-Mars-Earth Trajectories

Our search of E-V-M-E abort trajectories between 2014 and 2031 produced solutions in nearly all launch years. Figure 7 shows potential trajectories with a total time of flight less than 1000 days and a launch V_∞ of 4.5 km/s. As with the E-M-V-E cases, we searched for trajectories with launch V_∞ between 3.4 and 4.6 km/s using an increment of 0.1 km/s. We see in Figure 7 that trajectories exist with a time of flight less than 800 days in 2016, 2017, 2021 and 2023. A more detailed representation of the 2021 family of trajectories is shown in Figure 8. A number of trajectories exist in 2021, which require little, or no, ΔV. Unfortunately, the time of flight to Mars for these trajectories exceeds the 180-day limit. Due to the flyby of Venus occurring prior to

arrival at Mars, the E-V-M-E trajectory option always has a longer TOF to Mars than the 180-day constraint. As the proposed transport is designed to possess an artificial gravity environment, we have not dismissed all of the E-V-M-E options.

The best options for the E-V-M-E abort trajectories are listed in Table 7. Most of the options are free-returns, which do not require a ΔV. We note that the best cases for 2015 and 2016 require a ΔV of 0.9 and 0.7 km/s, respectively. From the trajectories listed in Table 7, we identify the 2015, 2017 and 2021 opportunities as potential abort options. Although the times of flight to Mars are all over 300 days, the total TOF to arrive at Earth for these trajectories are all less than 700 days. The 2021 opportunity is the best E-V-M-E alternative with a TOF to Mars of 323 days and a TOF to return to Earth of only 582 days. Table 8 presents the tether designs needed for the E-V-M-E abort trajectories. As most of the options are free-returns, there are no geometric constraints for the tether transport facility. We note that for both the 2015 and 2016 cases $m_T/m_p < 3$. The 2016 trajectory is not selected as a suitable option because the TOF for arriving at Earth is 761 days and the TOF to Mars is greater than 1 year.

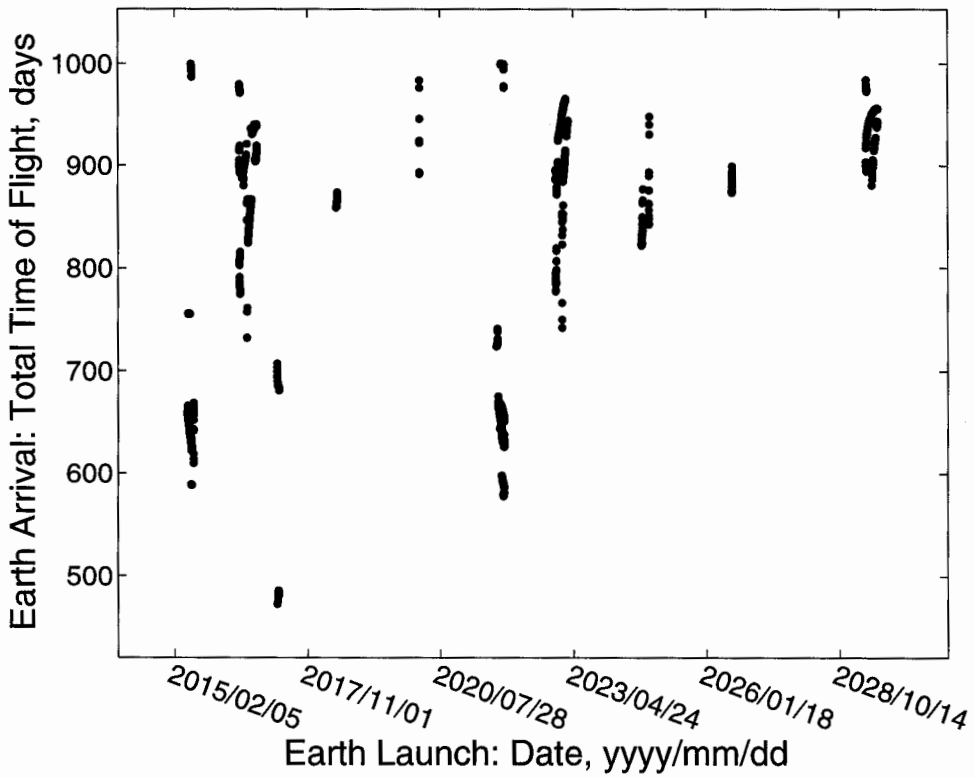

Figure 7 E-V-M-E trajectories found between 2014 and 2031 with a maximum time-of-flight of 1000 days. The minimum flyby altitude searched is 200 km with a launch V_∞ of 4.5 km/s and a maximum ΔV between Mars and Earth of 0.9 km/s.

Table 7: E-V-M-E abort options with a deep space maneuver

Launch Date, yyyy/mm/dd	Launch V_∞, km/s	Mars Arrival V_∞, km/s	Earth Arrival V_∞, km/s	Deep Space Maneuver, km/s	TOF to Mars,[a] days	TOF to Earth,[b] days
2015/06/12	**4.5**	**5.20**	**9.30**	**0.90**	**352**	**588**
2016/08/04	4.5	5.80	6.86	0.70	374	761
2017/03/29	**4.5**	**5.33**	**8.03**	**0.00**	**367**	**681**
2018/06/11	4.2	12.0	10.5	0.00	819	880
2020/02/29	4.3	9.13	12.15	0.01	579	897
2021/11/22	**4.5**	**5.42**	**6.48**	**0.00**	**323**	**582**
2023/01/30	4.5	7.17	7.05	0.00	630	766
2024/09/25	4.5	9.50	10.84	0.00	540	850
2026/07/31	4.5	12.5	13.1	0.00	521	886
2029/06/14	4.5	4.70	8.18	0.00	650	868

[a] TOF to Mars is the time of flight for E-V-M.
[b] TOF to Earth is time of flight for E-M-V-E.

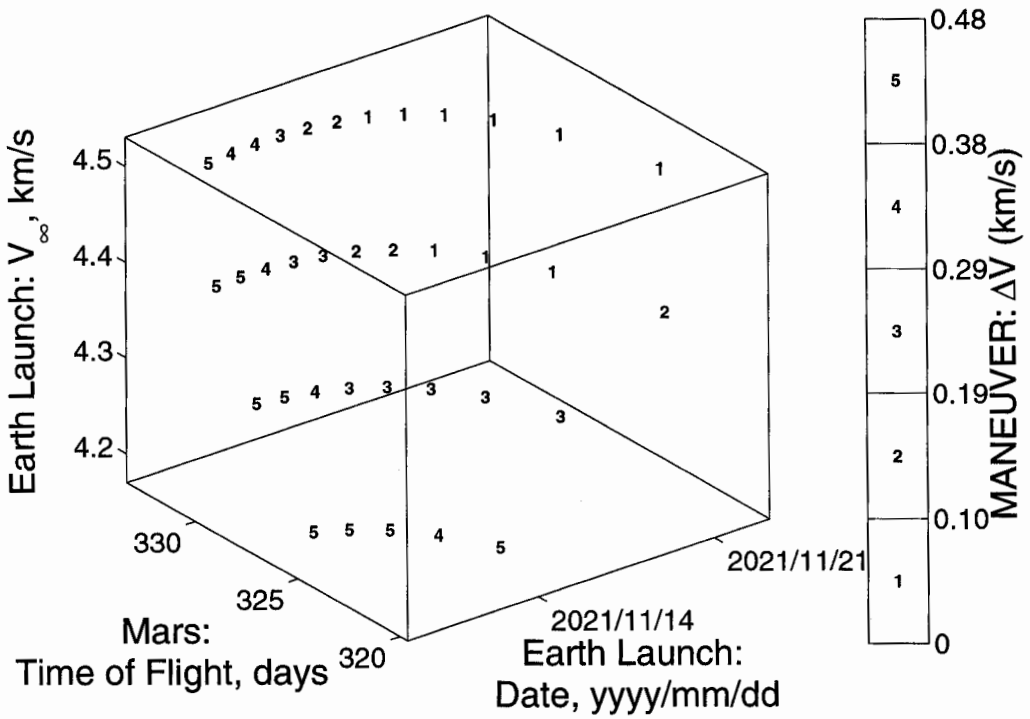

Figure 8 2021 E-V-M-E trajectory options with TOF < 600 days.

Table 8: Tether designs for E-V-M-E abort options

Launch Date, yyyy/mm/dd	Deep Space Maneuver, km/s	m_C/m_H	Tether Mass (m_T), Mg	Tether Length (L_C+L_H), km	m_T/m_H	m_T/m_p
2015/06/12	**0.90**	**0.44**	**38.0**	**231**	**0.62**	**2.9**
2016/08/04	0.70	0.44	23.5	146	0.39	2.3
2017/03/29	**0.00**	**0.44**	**a**	**a**	**a**	**a**
2018/06/11	0.00	0.44	a	a	a	a
2020/02/29	0.01	0.44	a	a	a	a
2021/11/22	**0.00**	**0.44**	**a**	**a**	**a**	**a**
2023/01/30	0.00	0.44	a	a	a	a
2024/09/25	0.00	0.44	a	a	a	a
2026/07/31	0.00	0.44	a	a	a	a
2029/06/14	0.00	0.44	a	a	a	a

[a] There are no geometric requirements for the tether when the deep space maneuver is zero.

DISCUSSION

Table 9 contains our best abort scenario trajectory options between 2014 and 2031. The opportunities in 2014, 2018, 2020 and 2026 closely match our mission constraints. Although the 2026 option has a Mars arrival V_∞ of 7.83 km/s, we have accepted this opportunity due to the trajectory's DSM of 0.91 km/s. In this instance the spinning tether can reduce the magnitude of the arrival V_∞ at Mars so that the entry conditions achieve the mission constraints. Although a DSM of 0.91 km/s is too large for the descent engines alone, the DSM might be realised via a combination of the tether rotation and descent engines. The E-M-E trajectories recommended for 2018 and 2020 require DSMs of 0.71 and 0.5 km/s, which can be achieved using the descent engines. The final preferred case in 2014 is a free-return trajectory and, therefore, the tethered transport's geometry is independent of the trajectory.

We note that most of the trajectory options listed in the table follow the E-M-E path. The only E-M-V-E case listed occurs in 2014, while E-V-M-E cases are recommended for 2015 and 2021. As noted previously, the E-V-M-E trajectory options violate the TOF design limits. We present free-return trajectory options for 2014 and 2021. The most difficult years for abort scenarios that meet our design constraints appear to be 2016, 2022, 2024 and 2028. We expect that combining the spinning tether system with the descent stage engines might make the options listed for 2016, 2022 and 2024 feasible. Of course, this would prevent the abort scenarios from being propellant-free.

Table 9: Selected abort options (with a deep space maneuver) for human missions to Mars

Launch Date, yyyy/mm/dd	Path	Launch V_∞, km/s	Mars Arrival V_∞, km/s	Earth Arrival V_∞, km/s	DSM, km/s	$\frac{m_T}{m_P}$	TOF to Mars, days	TOF to Earth, days
2014/01/13	**E-M-V-E**	**3.60**	**6.98**	**4.81**	**0.00**	**a**	**170**	**800**
2015/06/12	E-V-M-E	4.50	5.20	9.30	0.90	2.9	352	588
2016/02/28	E-M-E	3.45	7.58	4.79	1.20	4.0	125	778
2018/05/10	**E-M-E**	**3.90**	**7.09**	**5.06**	**0.71**	**2.3**	**187**	**759**
2020/07/27	**E-M-E**	**4.50**	**5.59**	**5.01**	**0.50**	**1.6**	**134**	**742**
2021/11/22	E-V-M-E	4.50	5.42	6.48	0.00	a	323	582
2022/09/12	E-M-E	4.52	4.94	4.90	1.01	3.3	171	753
2024/10/17	E-M-E	4.56	6.07	4.86	1.12	3.7	180	753
2026/11/21	**E-M-E**	**4.51**	**7.83**	**4.85**	**0.91**	**2.9**	**172**	**747**
2028/12/28	E-M-E	4.51	9.53	4.86	0.64	2.1	160	741

[a] There are no geometric requirements for the tether when the deep space maneuver is zero.

CONCLUSIONS

A minimum-mass, spinning tether transport can facilitate the propellant-free return of astronauts to Earth in the event of an aborted landing on Mars. We have identified abort scenarios in the years 2014, 2018, 2020 and 2026 that closely match the mission parameters of NASA's Design Reference Mission. Our minimum-mass tether design methodology enabled us to develop transport configurations for the abort scenarios with a tether-mass-to-propellant-mass ratio of less than 3. If the time-of-flight constraints are extended because the tether transport provides artificial gravity, then the Earth-Venus-Mars-Earth trajectory options become feasible. We have identified a good free-return E-V-M-E abort option in 2021. Relaxation of the constraints for human missions to Mars and improvements in tether strength-to-weight ratios may produce more abort options. The abort scenarios and artificial-gravity tether transports presented in this paper have the potential to play an important role in missions to Mars.

REFERENCES

[1] Hoyt, R. P. and Uphoff, C. W., "Cislunar Tether Transport System," *Journal of Spacecraft and Rockets*, Vol. 37, No. 2, 2000, pp. 177-186.

[2] Forward, R. and Nordley, G., "Mars-Earth Rapid Interplanetary Tether Transport (MERITT) System: Initial Feasibility Study," AIAA Paper 99-2839, 1999.

[3] Bogar, T. J., Bangham, M. E., Forward, R. L., Lewis, M. J., "Hypersonic Airplane Space Tether Orbital Launch (HASTOL) System: Interim Study Results," AIAA Paper 99-4802, 1999.

[4] Colombo, G., "The use of Tether for Payload Orbit Transfer," NASA, Report N82-26705, 1982.

[5] Cosmo, M. L. and Lorenzini, E. C., Eds., *Tethers in Space Handbook, 3rd ed.*, prepared for NASA/MSFC by the Smithsonian Astrophysical Observatory, Cambridge, MA, 1997.

[6] Tillotson, B., "Tether as Upper Stage for Launch to Orbit," *Third International Conference on Tethers in Space – Toward Flight*, Paper 89-1585-CA, San Francisco, CA, 1989.

[7] Puig-Suari, J., Longuski, J. M. and Tragesser, S. G., "A Tether Sling for Lunar and Interplanetary Exploration," *Acta Astronautica*, Vol. 36, 1995, pp. 291-295.

[8] Kuchnicki, S. N., Tragesser, S. G. and Longuski, J. M., "Dynamics of a Tether Sling," American Astronautical Society/AIAA Astrodynamics Specialist Conference, Paper AAS 97-605, Sun Valley, ID, 1997.

[9] Jokic, M. D. and Longuski, J. M., "Design of a Tether Sling for Human Transportation System between Earth and Mars," AIAA Paper 2002-4642, 2002.

[10]Pasca, M. and Lorenzini, E. C., "Collection of Martian Atmospheric Dust with a Low Altitude Tethered Probe," *Advances in the Astronautical Sciences*, Vol. 75, 1991, pp. 1121-1139.

[11]Pasca, M. and Lorenzini, E. C., "Optimization of a Low Altitude Tethered Probe for Martian Atmospheric Dust Collection," *Journal of the Astronautical Sciences*, Vol. 44, 1996, pp. 191-205.

[12]Walberg, G. D., "How Shall We Go to Mars? A Review of Mission Scenarios," *Journal of Spacecraft and Rockets*, Vol. 30, No.2, 1993, pp. 129-139.

[13]Wilson, S., "Fast Round Trip Mars Trajectories," AIAA Paper 90-2934, Aug. 1990.

[14]Hollister, W. M., "Mars Round Trip Trajectories," AIAA Paper 64-67, Aug. 1964.

[15]Ross, S., "Trajectory Design for Planetary Mission Analysis," Resent Developments in Space Flight Mechanics, Vol. 9, American Astronautical Society Science and Technology Ser., American Astronautical Society, Tarzana, CA, 1965, pp. 3-43.

[16]Sohn, R. L., "Manned Mars Trips Using Venus Flyby Modes," *Journal of Spacecraft and Rockets*, Vol. 3, No. 2, 1996, pp. 161-169.

[17]Battin, R. H., *An Introduction to the Mathematics and Methods of Astrodynamics*, AIAA Education Series, AIAA, New York, 1987, pp. 15-19, 431-436.

[18]Zubrin, R., *The Case for Mars*, 1st ed., Simon and Schuster, New York, 1997, pp. 75-101,113-132.

[19]Lyne, J. E., and Braun, R. D., "Flexible Strategies for Manned Mars Missions Using Aerobraking and Nuclear Thermal Propulsion," *Journal of the Astronautical Sciences*, Vol. 41, No. 3, 1993, pp. 339-347.

[20]Williams, S. N., and Longuski, J. M., "Low Energy Trajectories to Mars via Gravity Assist from Venus to Earth," *Journal of Spacecraft and Rockets*, Vol. 28, No. 4, 1991, pp. 486-488.

[21]Desai, P. N., Braun, R. D., and Powell, R. W., "Aspects of Parking Orbit Selection in a Manned Mars Mission," NASA TP-3256, Dec. 1992, p. 27.

[22]Hofman, S. J., and Kaplan, D. I. (eds.), "Human Exploration of Mars: The Reference Mission of the NASA Mars Exploration Study Team," NASA SP 6107, March 1997.

[23]Drake, B. G. (ed.), "Reference Mission Version 3.0 Addendum to the Human Exploration of Mars: The Reference Mission of the NASA Mars Exploration Study Team," NASA Rept. EX-98-036, June 1998.

[24]Munk, M. M., "Departure Energies, Trip Times and Entry Speeds for Human Mars Missions," American Astronautical Society, AAS Paper 99-103, Feb. 1999.

[25]Lyne, J. E., and Townsend, L. W., "Critical Need for a Swingby Return Option for Early Manned Missions," *Journal of Spacecraft and Rockets*, Vol. 35, No. 6, 1998, pp. 855-856.

[26]Lyne, J. E., Wercinki, P., Walberg, G. D., and Jits, R., "Mars Aerocapture Studies for the Design Reference Mission," American Astronautical Society, AAS Paper 98-110, Feb. 1998.

[27]Patel, M. R., Longuski, J. M., and Sims, J. A., "Mars Free Return Trajectories," *Journal of Spacecraft and Rockets*, Vol. 35, No. 3, 1998, pp. 350-354.

[28]Wolf, A. A., "Free Return Trajectories for Mars Missions," American Astronautical Society, AAS Paper 99-123, Feb. 1991.

[29]Okutsu, M., and Longuski, J. M., "Mars Free Returns vis Gravity Assist from Venus," *Journal of Spacecraft and Rockets*, Vol. 39, No. 1, 2002, pp. 31-36.

[30]Friedlander, A. L., Niehoff, J. C., Byrnes, D. V., and Longuski, J. M., "Circulating Transportation Orbits Between Earth and Mars," AIAA Paper 86-2009, Aug. 1986.

[31]Aldrin, B., "Cyclic Trajectory Concepts," SAIC presentation to the Interplanetary Rapid Transit Study Meeting, Jet Propulsion Laboratory, Pasadena, CA, Oct. 28, 1985.

[32]Byrnes, D. V., Longuski, J. M., and Aldrin, B., "Cycler Orbit Between Earth and Mars," *Journal of Spacecraft and Rockets*, Vol. 30, No. 3, 1993, pp. 334-336.

[33]Hoffman, S. J., Friedlander, A. L., and Nock, K. T., "Transportation Node Performance Comparison for a Sustained Manned Mars Base," AIAA Paper 86-2016, Aug. 1986.

[34]Bishop, R. H., Byrnes, D. V., Newman, D. J., Carr, C. E., and Aldrin, B., "Earth-Mars Transportation Opportunities: Promising Options for Interplanetary Transportation," American Astronautical Society/AIAA Astrodynamics Conference, Paper AAS 00-255, College Station, TX, Mar. 2000.

[35]Nock, K. T., "Cyclical Visits to Mars via Astronaut Hotels," Phase I Final Report, NASA Institute for Advanced Concepts, Universities Space Research Association Research Grant 07600-049, Nov. 30, 2000.

[36]Nock, K. T., and Friedlander, A. L., "Elements of a Mars Transportation System," *Acta Astronautica*, Vol. 15, No. 6/7, 1987, pp. 505-522.

[37]Aldrin, B., Byrnes, D., Jones, R., and Davis, H., "Evolutionary Space Transportation Plan for Mars Cycling Concepts," AIAA Paper 2001-4677, 2001.

[38]Chen, J. K., Landau, D. F., McConaghy, T. T., Masataka, O., Longuski, J. M., and Aldrin, B., "Trajectory Analysis and Design of Mars Cyclers: Preliminary Assessment," AIAA 2002-4422, Aug. 2001.

[39]McConaghy, T. T., Longuski, J. M. and Byrnes, D. V., "Analysis of a Broad Class of Earth-Mars Cycler Trajectories," AIAA/AAS Astrodynamics Specialist Conference, AIAA Paper 2002-4420, Monterey, CA, Aug. 5-8, 2002.

[40]Chen, K. J., McConaghy, T. T., Okutsu, M., and Longuski, J. M., "A Low-Thrust Version of the Aldrin Cycler," AIAA 2002-4421, Aug. 2002.

[41]Corless, R. M., Gonnet, G. H., Hare, D. E. G., Jeffrey, D. J., and Knuth, D. E., "On the Lambert W Function," *Advances in Computational Mathematics*, Vol. 5, pp. 329-359, 1996.

[42]George, L. E., and Kos, L. D., "Interplanetary Mission Design Handbook: Earth-to-Mars Mission Opportunities and Mars-to-Earth Return Opportunities 2009-2024," NASA/TM-1998-208533, July 1998.

[43]Rinderle, E. A., "Galileo User's Guide, Mission Design System, Satellite Tour Analysis and Design Subsystem," Jet Propulsion Laboratory, JPL Publication D-263, California Institute of Technology, Pasadena, CA, July 1986.

[44]Sauer, C. G., Jr., "MIDAS: Mission Design and Analysis Software for the Optimization of Ballistic Interplanetary Trajectories," *Journal of the Astronautical Sciences*, Vol. 37, No. 3, 1989, pp. 768-775.